

## Thermodynamics and Magnetic Properties of the Anisotropic 3D Hubbard Model

Jakub Imriška,<sup>1</sup> Mauro Iazzi,<sup>1</sup> Lei Wang,<sup>1</sup> Emanuel Gull,<sup>2</sup> Daniel Greif,<sup>3</sup> Thomas Uehlinger,<sup>3</sup> Gregor Jotzu,<sup>3</sup> Leticia Tarruell,<sup>3,4,5</sup> Tilman Esslinger,<sup>3</sup> and Matthias Troyer<sup>1</sup>

<sup>1</sup>*Theoretische Physik, ETH Zurich, 8093 Zurich, Switzerland*

<sup>2</sup>*University of Michigan, Ann Arbor, Michigan 48109, USA*

<sup>3</sup>*Institute for Quantum Electronics, ETH Zurich, 8093 Zurich, Switzerland*

<sup>4</sup>*LP2N UMR 5298, Université Bordeaux I, Institut d'Optique and CNRS, 33405 Talence, France*

<sup>5</sup>*ICFO-Institut de Ciències Fòniques, Mediterranean Technology Park, 08860 Castelldefels (Barcelona), Spain*

(Received 2 October 2013; revised manuscript received 17 February 2014; published 18 March 2014)

We study the anisotropic 3D Hubbard model with increased nearest-neighbor tunneling amplitudes along one direction using the dynamical cluster approximation and compare the results to a quantum simulation experiment of ultracold fermions in an optical lattice. We find that the short-range spin correlations are significantly enhanced in the direction with stronger tunneling amplitudes. Our results agree with the experimental observations and show that the experimental temperature is lower than the strong tunneling amplitude. We characterize the system by examining the spin correlations beyond neighboring sites and determine the distribution of density, entropy, and spin correlation in the trapped system. We furthermore investigate the dependence of the critical entropy at the Néel transition on anisotropy.

DOI: [10.1103/PhysRevLett.112.115301](https://doi.org/10.1103/PhysRevLett.112.115301)

PACS numbers: 67.85.-d, 71.10.Fd, 71.27.+a

The Hubbard model is one of the simplest condensed matter models incorporating the complex interplay between the itinerant and localized behavior of fermions on a lattice. Its phase diagram is expected to contain a number of interesting phases, such as pseudogap states, magnetic long-range order, and  $d$ -wave superconductivity [1–6]. Capturing the entire phase diagram theoretically has turned out to be a challenging task, where no unbiased numerical method exists in the interesting strongly correlated region. Furthermore, a detailed validation of theoretical results by comparison to measurements in real materials is often hindered by their structural complexity and limited knowledge of their system parameters.

In this context, the controlled setting of ultracold fermions in optical lattices offers the possibility to directly realize the Hubbard model [7,8] in an experiment and has allowed for studying the metal to Mott insulator crossover [9,10]. At half filling, magnetic correlations are expected to arise at lower temperatures, as a consequence of superexchange, and ultimately create a Néel phase characterized by long-range antiferromagnetic order. While this has so far not been accessed experimentally, short-range quantum magnetism has been observed in a recent experiment [11]. In particular, antiferromagnetic spin correlations on neighboring sites were measured using an anisotropic simple cubic lattice configuration, in which the tunneling along one direction was enhanced. In contrast to previous measurements, where a perturbative high-temperature expansion was sufficient to describe the system [12–14], understanding this new quantum simulation experiment requires a more sophisticated theoretical approach. Open

questions included the influence of the anisotropy on the temperature of the system and the entropy distribution in the trap.

Although the thermodynamics, spin correlations, and Néel transition temperature for the isotropic 3D Hubbard model have been calculated with different numerical methods [15–19], the anisotropic Hubbard model was only studied in the Heisenberg limit [20], where the Néel temperature was found to drop continuously to zero as the interchain coupling decreases. However, the experiment [11] is carried out at weak to intermediate interaction strength, where charge fluctuations cannot be ignored. There, the dependence of the Néel temperature on anisotropy and the behavior of the strength, range, and orientation of spin correlations are unknown. In this Letter we perform a quantitative analysis of the anisotropic Hubbard model using the dynamical cluster approximation (DCA) [21] and compare it to the results of a quantum simulation experiment using ultracold fermions in an optical lattice [11]. To take into account the trapping potential in the experiment, we use the local density approximation (LDA), which has been proven to be accurate in the temperature region relevant for comparison with the experiment [22–24]. The calculated and experimentally measured spin correlations are found to be in good agreement for temperatures down to the tunneling energy, showing a strong enhancement for large tunneling anisotropies. However, the calculated critical entropies for long-range magnetic order in the anisotropic homogeneous system are found to be below the maximum value of the isotropic case at  $U = 8t$ .

The Hamiltonian of the anisotropic Hubbard model on a cubic lattice is given by

$$\begin{aligned} \hat{H} = & -t \sum_{\mathbf{r}, \sigma} (\hat{c}_{\mathbf{r}+\mathbf{e}_x, \sigma}^\dagger \hat{c}_{\mathbf{r}\sigma} + \text{H.c.}) \\ & - t' \sum_{\mathbf{r}, \sigma} (\hat{c}_{\mathbf{r}+\mathbf{e}_y, \sigma}^\dagger \hat{c}_{\mathbf{r}\sigma} + \hat{c}_{\mathbf{r}+\mathbf{e}_z, \sigma}^\dagger \hat{c}_{\mathbf{r}\sigma} + \text{H.c.}) \\ & + U \sum_{\mathbf{r}} \hat{n}_{\mathbf{r}\uparrow} \hat{n}_{\mathbf{r}\downarrow} - \mu \sum_{\mathbf{r}, \sigma} \hat{n}_{\mathbf{r}\sigma}, \end{aligned} \quad (1)$$

where  $\hat{c}_{\mathbf{r}\sigma}^\dagger$  ( $\hat{c}_{\mathbf{r}\sigma}$ ) creates (annihilates) a fermion at lattice site  $\mathbf{r}$  with spin  $\sigma \in \{\uparrow, \downarrow\}$ ;  $\hat{n}_{\mathbf{r}\sigma} \equiv \hat{c}_{\mathbf{r}\sigma}^\dagger \hat{c}_{\mathbf{r}\sigma}$  denotes the occupation number operator;  $\mathbf{e}_i$  denotes the unit vector (setting the lattice spacing to 1) along the direction  $i \in \{x, y, z\}$ . The system has the tunneling amplitude  $t$  along the  $x$  axis and  $t'$  in the directions  $y, z$  as shown in Fig. 1(a). The repulsive on-site interaction energy is denoted by  $U > 0$  and the chemical potential by  $\mu$ . The ratio  $t/t'$  will be referred to as the anisotropy of the system. In this Letter, we consider  $t/t' \geq 1$ , covering the range from an isotropic 3D system to weakly coupled 1D chains.

We study the physical properties of Eq. (1) with the DCA, using the numerically exact continuous time auxiliary field quantum Monte Carlo impurity solver [25,26]. The results were extrapolated in cluster size to obtain results in the thermodynamic limit [17,27].

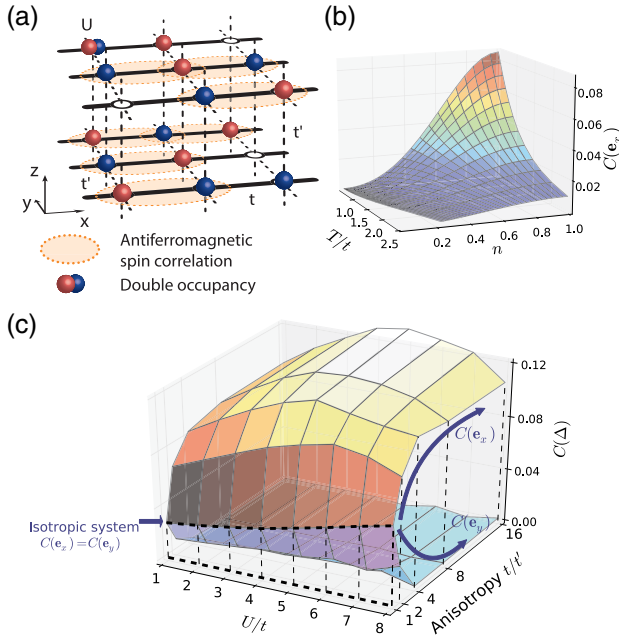


FIG. 1 (color online). (a) Sketch of the anisotropic 3D Hubbard model according to Eq. (1). (b) NN spin correlation  $C(\mathbf{e}_x)$  versus filling and temperature for  $t/t' = 7.36$ ,  $U = 1.4375t$  in a homogeneous system. (c) NN spin correlation along the strong tunneling  $C(\mathbf{e}_x)$  (upper surface) and in the transverse direction  $C(\mathbf{e}_y)$  (lower surface) for a homogeneous system at half filling and  $T = 0.5t$  as a function of anisotropy and interaction strength.

We have calculated the thermodynamic properties including energy ( $e$ ) and density ( $n$ ) per site at a given chemical potential  $\mu$  and the inverse temperature  $\beta = 1/T$  (setting  $k_B = 1$ ). The entropy per site  $s(\beta)$  is obtained by numerical integration

$$s(\beta) = s(\beta_0) + f(\beta)\beta - f(\beta_0)\beta_0 - \int_{\beta_0}^{\beta} f(\beta') d\beta', \quad (2)$$

with  $f(\beta) = e(\beta) - \mu n(\beta)$ . Tabulated equation of state data and technical details may be found in the Supplemental Material [28].

In addition to the thermodynamic properties, we calculate the equal-time spin correlation function

$$C(\Delta) = -\frac{2}{L} \sum_{\mathbf{r}} \langle \hat{S}_{\mathbf{r}}^z \hat{S}_{\mathbf{r}+\Delta}^z \rangle, \quad (3)$$

where  $\hat{S}_{\mathbf{r}}^z = \frac{1}{2}(\hat{n}_{\mathbf{r}\uparrow} - \hat{n}_{\mathbf{r}\downarrow})$ ,  $\Delta$  is a lattice vector, and  $L$  is the number of sites. Figure 1(b) shows  $C(\mathbf{e}_x)$  for various fillings and temperatures at fixed  $t/t' = 7.36$  and  $U = 1.4375t$ , which was used in the experiment of Ref. [11]. Antiferromagnetic correlations between nearest neighbors (NNs) correspond to positive values of  $C(\mathbf{e}_x)$ . The signal is greatly enhanced for  $T \lesssim t$  and close to half filling. At fixed temperature and interaction strength, the NN spin correlation along the longitudinal direction  $C(\mathbf{e}_x)$  is enhanced with anisotropy  $t/t'$ , while the correlation along the transverse direction  $C(\mathbf{e}_y)$  is suppressed, see Fig. 1(c).  $T/t'$  is higher in the anisotropic case and thus the development of spin correlations in the transverse direction  $y$  is suppressed. At the same time  $C(\mathbf{e}_x)$  is enhanced because singlet formation is facilitated by the effective lowering of dimensionality [29]. This in turn is caused by the difference in the relevant energy scales:  $T$  and  $t$  are of the same order but an order of magnitude larger than  $t'$ .

The quantum simulation experiment is performed as described in detail in Ref. [11] using a balanced spin-mixture of the  $m_F = -9/2, -7/2$  sublevels of the  $F = 9/2$  hyperfine manifold of  $^{40}\text{K}$ . About 60 000 fermions are prepared at 10% of the Fermi temperature in a harmonic optical dipole trap. The gas is then heated to control the entropy per particle  $S_{\text{in}}/N$  in the dipole trap. This is measured using fits to a Fermi-Dirac distribution. After setting the  $s$ -wave scattering length to 106(1) Bohr radii, an anisotropic cubic optical lattice operating at a wavelength of  $\lambda = 1064$  nm is turned on using an  $S$ -shaped ramp lasting 200 ms. The parameters of the Hubbard model describing the final lattice configuration are computed using Wannier functions.

In order to detect the number of singlets and triplets consisting of two neighboring atoms with opposite spins, we suddenly ramp to a deep simple cubic lattice, suppressing all tunnelings. A magnetic field gradient is then used to induce coherent oscillations between singlet and triplet states. Subsequently, we merge neighboring sites

adiabatically using a tunable-geometry optical lattice [30] and detect the number of double occupancies in the lowest band created by merging. The difference between the fraction of atoms detected in a singlet ( $p_s$ ) or triplet ( $p_t$ ) configuration can be used to compute the spin correlator

$$-\langle S_{\mathbf{r}}^x S_{\mathbf{r}+\mathbf{e}_x}^x \rangle - \langle S_{\mathbf{r}}^y S_{\mathbf{r}+\mathbf{e}_x}^y \rangle = (p_s - p_t)/2, \quad (4)$$

which is equal to  $C(\mathbf{e}_x)$  given the SU(2) invariance of the Hubbard model, Eq. (1).

**Results and discussions.**—Figure 2(a) shows the calculated and experimental NN spin correlation versus anisotropy  $t/t'$ ; owing to the experimental realization, the interaction  $U/t$  decreases for larger anisotropies in this scan. We find good agreement between the DCA + LDA calculation and the experimental data assuming an entropy per particle  $S/N$  in the range of 1.4 to 1.8. For anisotropies  $\gtrsim 5$  the experiment enters a regime where corrections to the single band Hubbard model, Eq. (1), may start to play a role in the shallow optical lattice [31]. Close to the isotropic limit, the second order high-temperature series expansion (HTSE) with  $S/N = 1.7$  describes the data well. For increasing anisotropies, the HTSE becomes unreliable as the expansion parameter  $\beta t$  reaches 1. The inset of Fig. 2(a) shows that the introduction of the anisotropy leads to a situation where the temperature becomes comparable to or lower than the strong tunnel coupling  $t$ . The average  $C(\mathbf{e}_x)$  increases monotonically with anisotropy, which is a consequence of both the enhancement of correlations for a given  $\beta t$  and additionally the increasing  $\beta t$ .

For a fixed anisotropy  $t/t' = 7.36$ , Fig. 2(b) shows the trap averaged  $C(\mathbf{e}_x)$  versus entropy per particle (for the experimental data the horizontal axis denotes the initial entropy per particle measured before loading into the lattice). Without any free parameters and assuming no heating, we find very good agreement for entropies of  $1.4k_B$  and above, showing that magnetic effects in the Hubbard model can be accurately studied in this regime. For lower entropies, the experimentally measured spin correlation does not increase further, deviating from the theoretical prediction. This suggests that additional heating may have occurred during the optical lattice loading process, or the system may not have fully equilibrated in the lattice for the lowest initial entropies. This is an important outcome of this study not deducible from the experimental data alone. A similar situation is found in previous studies of dimerized and simple cubic optical lattices [11,13]. The inset of Fig. 2(b) shows a comparison at a different anisotropy  $t/t' = 4.21$ , where similar agreement at high entropies and deviations at low entropies are found. The observed heating, which varies depending on the system parameters, may be caused by nonadiabaticity with respect to changes of the local Hamiltonian, or may be due to the expected long time scale of density redistribution within the harmonic trap [32].

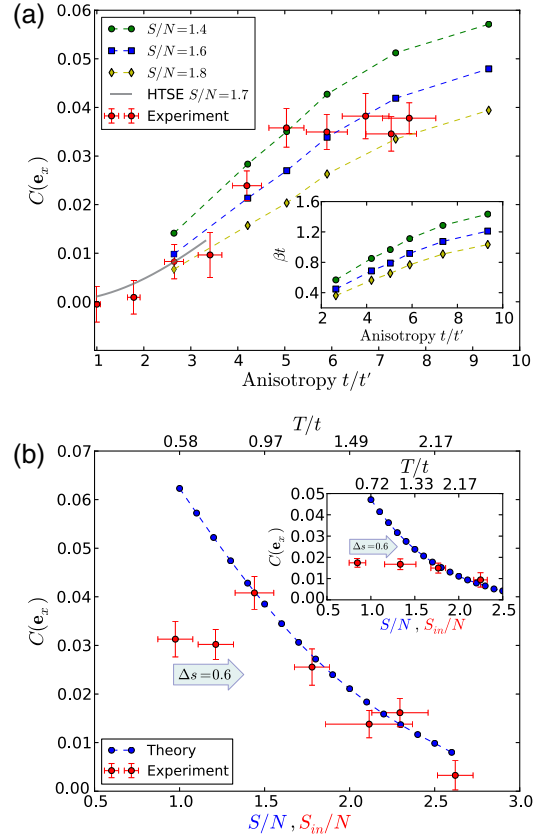


FIG. 2 (color online). Comparison of the calculated spin correlations from DCA + LDA calculation with the experiment. (a) NN spin correlation for different anisotropies and interaction strengths. The entropy per particle before loading into the lattice is below 1.0 in the experiment. For increasing anisotropy the interaction  $U/t$  decreases from 16.2 to 0.975. Detailed parameters are listed in the Supplemental Material [28]. Theoretical calculations with different entropies per particle are shown as symbols connected by dashed lines. The solid line shows HTSE results with  $S/N = 1.7$ . The inset shows the inverse temperature  $\beta t$  versus anisotropy used in the DCA + LDA calculations. (b) NN spin correlation as a function of entropy per particle for  $t/t' = 7.36$  and  $U = 1.4375t$ . The experimental data are plotted as a function of the initial  $S/N$  before loading into the lattice, and the dashed curve is the theoretical prediction. The upper axis denotes the corresponding temperature determined from the DCA + LDA calculation. For the lowest initial entropies the measured spin correlation deviates from the expected value. These experimental data points agree with an approximate entropy increase of 0.6 possibly caused by heating during lattice loading. The inset shows a comparison with the experiment at a different set of parameters ( $t/t' = 4.21$ ,  $U = 2.98t$ ). There, additional heating may have occurred below 1.8.

The upper horizontal axis of Fig. 2(b) shows the temperature used in the DCA + LDA calculations. For the lowest entropy  $S/N = 1.4$ , where the experimentally measured spin correlator matches the theoretical value, the temperature is found to be  $T \approx 0.88t$ . An anisotropic 3D system prepared at temperatures between the strong and weak exchange energy along and between the chains effectively

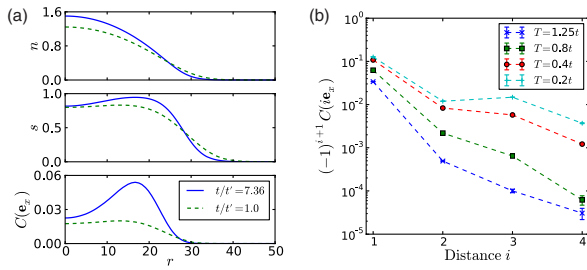


FIG. 3 (color online). (a) The distribution of density, entropy, and NN spin correlation per site in the harmonic trap versus distance from the center. The simulation is done with  $U = 1.4375t$  with the trap averaged entropy  $S/N = 1.6$ . The chemical potential and trapping frequency are chosen such that the filling is  $n = 1$  at the trap center and  $N = 50\,000$  for both anisotropy ratios. (b) Extrapolated spin correlations as a function of distance along the  $x$  axis in the paramagnetic phase for  $t/t' = 7.36$ ,  $U = 1.44t$ , and half filling for different temperatures.

realizes an array of 1D systems in global thermodynamic equilibrium—in contrast to an array of decoupled 1D chains, where the thermalization is hindered by negligible tunneling between the 1D chains. It provides thus a viable system for an experimental study with controllable parameters of the low-temperature regime of the Hubbard model in effectively one dimension [33] at currently accessible experimental entropies.

Figure 3(a) shows the calculated distribution of the density, entropy, and NN spin correlation in the trap for the isotropic ( $t/t' = 1$ ) and anisotropic ( $t/t' = 7.36$ ) Hubbard model with the same  $U/t$ , particle number, and entropy per particle. In order to display the density and entropy redistribution, we tune in each case the trapping potential to obtain the filling  $n = 1$  in the trap center and to obtain the same total atom number [34]. The corresponding temperatures are  $T = 0.95t$  and  $T = 0.58t$ , respectively [35]. Owing to qualitatively similar equations of state between the isotropic and anisotropic case at fixed tunneling  $t$ , we find a very similar behavior for both the density and entropy distribution in the trap. This is in contrast with the dimerized lattice examined in Ref. [11], which has an energy gap. In Fig. 3(a) the NN spin correlations are more pronounced for large anisotropy when comparing to the isotropic case, similar to the results in Fig. 1(c). To further characterize the state realized in the experiment, we compute the spin correlation beyond NNs along the  $x$  direction, shown in Fig. 3(b). It shows an alternating sign with distance, confirming the presence of antiferromagnetic spin correlations [36]. At large distances the spin correlations are expected to decay exponentially, as the chosen temperatures are above the critical value of the Néel transition. For the experimentally accessible temperatures, already the next-nearest-neighbor correlations are calculated to be below the experimental resolution.

Finally, we address the question of how the introduction of anisotropy affects the Néel transition in a 3D half-filled

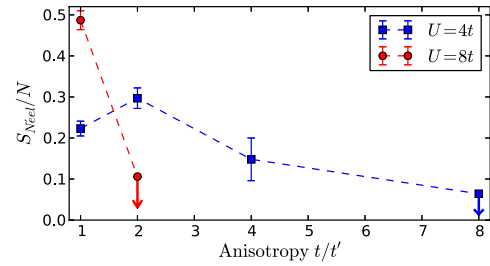


FIG. 4 (color online). Critical entropy per particle  $S(T_{\text{Neél}})/N$  at the Néel transition versus anisotropy for two different interactions at half filling. The data points shown with an arrow are upper bounds owing to the difficulty of obtaining the extrapolated  $T_{\text{Neél}}$  or a reliable  $s(T)$  down to the extrapolated transition temperature.

lattice. Figure 4 shows the calculated critical entropy at the Néel transition for different anisotropies. The critical entropy at  $U = 4t$  shows a nonmonotonic behavior as a function of anisotropy [37]. We explain this by the reduction of the total bandwidth  $W = 4(t + 2t')$  and thus by the effective increase of the interaction strength ( $U/W$ ) towards the optimal value  $U/W \approx 2/3$  for the isotropic system [17]. Consistent with our simple argument, the curve for  $U = 8t$  decays monotonically. We find that the introduction of anisotropy does not enhance the critical entropy over the optimum value [ $S/N \approx 0.487(23)$  in the present study] reached at  $U = 8t$  for the isotropic case.

The estimate of the Néel temperature was obtained for a set of clusters within the DCA simulation by looking for the divergence of the static antiferromagnetic spin susceptibility [21]; see details in the Supplemental Material [28].  $T_{\text{Neél}}$  was then obtained by extrapolation in cluster size as suggested in Refs. [16] and [38]. Figure 4 shows  $s(T_{\text{Neél}})$  with curve  $s(T)$  integrated within the paramagnetic phase. Our results for the isotropic case,  $T_{\text{Neél}}/t = 0.1955(25)$  for  $U = 4t$  and  $T_{\text{Neél}}/t = 0.3595(83)$  for  $U = 8t$ , are consistent with previous studies [15,16]. Both estimates are slightly above the estimates  $T_{\text{Neél}}/t < 0.17$ ,  $T_{\text{Neél}}/t = 0.3325(65)$  obtained by diagrammatic determinantal Monte Carlo calculations on larger lattices for  $U = 4t$  and  $U = 8t$ , respectively [19].

**Conclusions.**—We have computed the properties of the 3D anisotropic Hubbard model in the regime accessed by the quantum simulation experiment. Short-range spin correlations were shown to be enhanced by anisotropy, even when the critical entropy at the Néel temperature is reduced. Our theoretical results show good agreement with our experiments, allowing us to characterize this system in detail. In particular, using the nearest-neighbor spin correlation as a thermometer, the experimentally realized temperature was found to reach values below the strong tunneling amplitude. Given the access to effectively one-dimensional Hubbard chains featuring spin order, the tunability of an optical lattice system may be used to probe their excitation dynamics or the crossover from 1D to higher

dimensions [33]. Long-range order is obtained when the entropy in the center of the trap [see Fig. 3(a)] is lower than the critical entropy shown in Fig. 4. A highly anisotropic configuration is shown to be unfavorable for experiments aiming at the realization of the ordered state, despite displaying greatly enhanced short-range correlations.

We thank Jan Gukelberger, Peter Staar, Michael Messer, and James LeBlanc for useful discussions. This work was supported by the ERC Advanced Grants SIMCOFE and SQMS, the Swiss National Competence Center in Research QSIT, and the Swiss National Science Foundation. The calculations used a code based on the ALPS libraries [39,40] and were performed on the Brutus cluster at ETH Zurich.

*Note added.*—Recently, we became aware of a related finite temperature study of the 1 D Hubbard model [41].

- 
- [1] T. Maier, M. Jarrell, T. Pruschke, and J. Keller, *Phys. Rev. Lett.* **85**, 1524 (2000).
- [2] C. Huscroft, M. Jarrell, T. Maier, S. Moukouri, and A. N. Tahvildarzadeh, *Phys. Rev. Lett.* **86**, 139 (2001).
- [3] T. A. Maier, M. Jarrell, T. C. Schulthess, P. R. C. Kent, and J. B. White, *Phys. Rev. Lett.* **95**, 237001 (2005).
- [4] E. Gull, O. Parcollet, and A. J. Millis, *Phys. Rev. Lett.* **110**, 216405 (2013).
- [5] D. J. Scalapino, *Handbook of High-Temperature Superconductivity: Theory and Experiment* (Springer, New York, 2007), Chap. 13.
- [6] D. Zanchi and H. J. Schulz, *Phys. Rev. B* **54**, 9509 (1996).
- [7] T. Esslinger, *Annu. Rev. Condens. Matter Phys.* **1**, 129 (2010).
- [8] M. Lewenstein, A. Sanpera, V. Ahufinger, B. Damski, A. Sen, and U. Sen, *Adv. Phys.* **56**, 243 (2007).
- [9] R. Jördens, N. Strohmaier, K. Günter, H. Moritz, and T. Esslinger, *Nature (London)* **455**, 204 (2008).
- [10] U. Schneider, L. Hackermüller, S. Will, T. Best, I. Bloch, T. A. Costi, R. W. Helmes, D. Rasch, and A. Rosch, *Science* **322**, 1520 (2008).
- [11] D. Greif, T. Uehlinger, G. Jotzu, L. Tarruell, and T. Esslinger, *Science* **340**, 1307 (2013).
- [12] R. Jördens, L. Tarruell, D. Greif, T. Uehlinger, N. Strohmaier, H. Moritz, T. Esslinger, L. De Leo, C. Kollath, A. Georges, V. Scarola, L. Pollet, E. Burovski, E. Kozik, and M. Troyer, *Phys. Rev. Lett.* **104**, 180401 (2010).
- [13] D. Greif, L. Tarruell, T. Uehlinger, R. Jördens, and T. Esslinger, *Phys. Rev. Lett.* **106**, 145302 (2011).
- [14] T. Uehlinger, G. Jotzu, M. Messer, D. Greif, W. Hofstetter, U. Bissbort, and T. Esslinger, *Phys. Rev. Lett.* **111**, 185307 (2013).
- [15] R. Staudt, M. Dzierzawa, and A. Muramatsu, *Eur. Phys. J. B* **17**, 411 (2000).
- [16] P. R. C. Kent, M. Jarrell, T. A. Maier, and T. Pruschke, *Phys. Rev. B* **72**, 060411 (2005).
- [17] S. Fuchs, E. Gull, L. Pollet, E. Burovski, E. Kozik, T. Pruschke, and M. Troyer, *Phys. Rev. Lett.* **106**, 030401 (2011).
- [18] T. Paiva, Y. L. Loh, M. Randeria, R. T. Scalettar, and N. Trivedi, *Phys. Rev. Lett.* **107**, 086401 (2011).
- [19] E. Kozik, E. Burovski, V. W. Scarola, and M. Troyer, *Phys. Rev. B* **87**, 205102 (2013).
- [20] C. Yasuda, S. Todo, K. Hukushima, F. Alet, M. Keller, M. Troyer, and H. Takayama, *Phys. Rev. Lett.* **94**, 217201 (2005).
- [21] T. Maier, M. Jarrell, T. Pruschke, and M. H. Hettler, *Rev. Mod. Phys.* **77**, 1027 (2005).
- [22] V. W. Scarola, L. Pollet, J. Oitmaa, and M. Troyer, *Phys. Rev. Lett.* **102**, 135302 (2009).
- [23] Q. Zhou and T.-L. Ho, *Phys. Rev. Lett.* **106**, 225301 (2011).
- [24] S. Chiesa, C. N. Varney, M. Rigol, and R. T. Scalettar, *Phys. Rev. Lett.* **106**, 035301 (2011).
- [25] E. Gull, P. Werner, O. Parcollet, and M. Troyer, *Europhys. Lett.* **82**, 57003 (2008).
- [26] E. Gull, P. Staar, S. Fuchs, P. Nukala, M. S. Summers, T. Pruschke, T. C. Schulthess, and T. Maier, *Phys. Rev. B* **83**, 075122 (2011).
- [27] T. A. Maier and M. Jarrell, *Phys. Rev. B* **65**, 041104 (2002).
- [28] See Supplemental Material at <http://link.aps.org/supplemental/10.1103/PhysRevLett.112.115301> for details of the numerical methods, the experimental parameters, and the critical temperatures.
- [29] E. V. Gorelik, D. Rost, T. Paiva, R. Scalettar, A. Klümper, and N. Blümer, *Phys. Rev. A* **85**, 061602 (2012).
- [30] L. Tarruell, D. Greif, T. Uehlinger, G. Jotzu, and T. Esslinger, *Nature (London)* **483**, 302 (2012).
- [31] A. Georges, in *Ultra-cold Fermi Gases*, Proceedings of the International School of Physics “Enrico Fermi” Vol. 164, edited by M. Inguscio, W. Ketterle, and C. Salomon (IOS Press, Amsterdam, 2007), p. 477.
- [32] T. Uehlinger, G. Jotzu, M. Messer, D. Greif, W. Hofstetter, U. Bissbort, and T. Esslinger, *Phys. Rev. Lett.* **111**, 185307 (2013).
- [33] T. Giamarchi, *Quantum Physics in One Dimension* (Clarendon, Oxford, 2003).
- [34] The profiles for the experimental setting may be found in Ref. [28].
- [35]  $T/t$  is lower in the anisotropic case because of reduction of the total bandwidth.
- [36] In Fig. 3(b) we find  $|C(3\mathbf{e}_x)| > |C(2\mathbf{e}_x)|$  for  $T = 0.2t$ , which is a feature inherited from the half-filled noninteracting system on the cubic lattice, where spin correlations at even Manhattan distances vanish.
- [37] Our particular interest was the search for the optimal parameters  $U/t$  and  $t/t'$  in terms of largest  $S_{\text{Neel}}/N$ . For that reason we did not study the low  $U/t$  regime, where  $T_{\text{Neel}}$  in the isotropic case is much smaller than the critical temperature at  $U/t = 8$ .
- [38] For  $t = t'$  our model is part of the universality class of the 3D  $S = 1/2$  Heisenberg model and for  $t \neq t'$  it belongs to the classical 3D Heisenberg universality class, both of which have a critical exponent of  $\nu \approx 0.71$  [A. W. Sandvik, *Phys. Rev. Lett.* **80**, 5196 (1998)].
- [39] A. Albuquerque, F. Alet, P. Corboz, P. Dayal, A. Feiguin, S. Fuchs, L. Gamper, E. Gull, S. Gurtler, A. Honecker, R. Igarashi, M. Kormer, A. Kozhevnikov, A. Lauchli, S. Manmana, M. Matsumoto, I. McCulloch, F. Michel, R. Noack, G. Pawłowski *et al.*, *J. Magn. Magn. Mater.* **310**, 1187 (2007).
- [40] B. Bauer, L. D. Carr, H. G. Evertz, A. Feiguin, J. Freire, S. Fuchs, L. Gamper, J. Gukelberger, E. Gull, S. Guertler, A. Hehn, R. Igarashi, S. V. Isakov, D. Koop, P. N. Ma, P. Mates, H. Matsuo, O. Parcollet, G. Pawłowski, J. D. Picon *et al.*, *J. Stat. Mech.* (2011), P05001.
- [41] B. Sciolla, A. Tokuno, S. Uchino, B. Peter, T. Giamarchi, and C. Kollath, *Phys. Rev. A* **88**, 063629 (2013).